

This article was downloaded by: [Georgia Tech Library]

On: 31 October 2014, At: 16:58

Publisher: Taylor & Francis

Informa Ltd Registered in England and Wales Registered Number: 1072954 Registered office: Mortimer House, 37-41 Mortimer Street, London W1T 3JH, UK



International Journal of Control

Publication details, including instructions for authors and subscription information:
<http://www.tandfonline.com/loi/tcon20>

Output feedback sliding mode control for a linear multi-compartment lung mechanics system

Saing Paul Hou^a, Nader Meskin^a & Wassim M. Haddad^b

^a Electrical Engineering Department, Qatar University, Doha, Qatar

^b School of Aerospace Engineering, Georgia Institute of Technology, Atlanta, GA 30332, USA
Accepted author version posted online: 28 Feb 2014. Published online: 25 Mar 2014.

To cite this article: Saing Paul Hou, Nader Meskin & Wassim M. Haddad (2014) Output feedback sliding mode control for a linear multi-compartment lung mechanics system, International Journal of Control, 87:10, 2044-2055, DOI: [10.1080/00207179.2014.898864](https://doi.org/10.1080/00207179.2014.898864)

To link to this article: <http://dx.doi.org/10.1080/00207179.2014.898864>

PLEASE SCROLL DOWN FOR ARTICLE

Taylor & Francis makes every effort to ensure the accuracy of all the information (the "Content") contained in the publications on our platform. However, Taylor & Francis, our agents, and our licensors make no representations or warranties whatsoever as to the accuracy, completeness, or suitability for any purpose of the Content. Any opinions and views expressed in this publication are the opinions and views of the authors, and are not the views of or endorsed by Taylor & Francis. The accuracy of the Content should not be relied upon and should be independently verified with primary sources of information. Taylor and Francis shall not be liable for any losses, actions, claims, proceedings, demands, costs, expenses, damages, and other liabilities whatsoever or howsoever caused arising directly or indirectly in connection with, in relation to or arising out of the use of the Content.

This article may be used for research, teaching, and private study purposes. Any substantial or systematic reproduction, redistribution, reselling, loan, sub-licensing, systematic supply, or distribution in any form to anyone is expressly forbidden. Terms & Conditions of access and use can be found at <http://www.tandfonline.com/page/terms-and-conditions>

Output feedback sliding mode control for a linear multi-compartment lung mechanics system

Saing Paul Hou^a, Nader Meskin^{a,*} and Wassim M. Haddad^b

^aElectrical Engineering Department, Qatar University, Doha, Qatar; ^bSchool of Aerospace Engineering, Georgia Institute of Technology, Atlanta, GA 30332, USA

(Received 9 June 2013; accepted 23 February 2014)

In this paper, we develop a sliding mode control architecture to control lung volume and minute ventilation in the presence of modelling system uncertainties. Since the applied input pressure to the lungs is, in general, nonnegative and cannot be arbitrarily large, as not to damage the lungs, a sliding mode control with bounded nonnegative control inputs is proposed. The controller only uses output information (i.e., the total volume of the lungs) and automatically adjusts the applied input pressure so that the system is able to track a given reference signal in the presence of parameter uncertainty (i.e., modelling uncertainty of the lung resistances and lung compliances) and system disturbances. Controllers for both matched and unmatched uncertainties are presented. Specifically, a Lyapunov-based approach is presented for the stability analysis of the system and the proposed control framework is applied to a two-compartment lung model to show the efficacy of the proposed control method.

Keywords: sliding mode control; multi-compartment lung system; output feedback control

1. Introduction

Human lungs are vulnerable to critical illness and as a consequence, respiratory failure is common for patients in intensive care units. Respiratory failure is the loss of the respiratory system's ability to maintain oxygen and/or carbon dioxide within normal ranges. In this case, mechanical ventilation is needed to provide an adequate exchange of oxygen and carbon dioxide (CO₂) in order for the organs to function normally. However, mechanical ventilation can cause lung injury and worsen patient outcome if the applied ventilation pressure is too high. The challenge of modern mechanical ventilation is, therefore, to provide the desired blood levels of CO₂ and oxygen with limited pressure so as to avoid damaging the lungs.

The earliest primary modes of ventilation can be classified, approximately, as volume-controlled or pressure-controlled (Tobin, 1994). In volume-controlled ventilation, the lungs are inflated (by the mechanical ventilator) to a specified volume and then allowed to passively deflate to the baseline volume. The mechanical ventilator controls the volume of each breath and the number of breaths per minute. In pressure-controlled ventilation, the lungs are inflated to a given peak pressure. The ventilator controls this peak pressure as well as the number of breaths per minute. Although, conventional mechanical ventilators only control the volume or input pressure during the inspiration phase, and the expiration phase is passive (i.e., the input pressure during the expiration phase is the atmospheric

pressure), some mechanical ventilators maintain a positive input pressure during the expiration phase to prevent early airway closure and alveolar collapse at the end of expiration (McLuckie, 2004; Medoff et al., 2000). Control architectures where positive input pressures are applied during both inspiration and expiration are proposed in Li and Haddad (2013) and Volyanskyy, Haddad, and Bailey (2011). Specifically, a reference airflow pattern is specified by the clinician and the objective of the controllers is to apply an appropriate input pressure so that the total lung volume tracks the reference pattern during the inspiration and expiration phases.

The primary determinant of the level of CO₂ in the blood is minute ventilation, which is defined as the tidal volume (the volume of each breath) multiplied by the number of breaths per minute (Martin, 1987; West, 2008). With volume-controlled ventilation, both tidal volume and the number of breaths are determined by the machine (the ventilator), and typically, the tidal volumes and breaths per minute are selected by the clinician caring for the patient. In pressure-controlled ventilation, the tidal volume is not directly controlled. The ventilator determines the pressure that inflates the lungs and the tidal volume is proportional to this driving pressure and the compliance or 'stiffness' of the lungs. Consequently, the minute ventilation is not directly controlled by the ventilator and any change in lung compliance (such as improvement or deterioration in the underlying lung pathology) can result in changes in tidal

*Corresponding author. Email: nader.meskin@qu.edu.qa

volume, minute ventilation, and ultimately, the blood concentration of CO₂.

The common theme in modern ventilation control algorithms is the use of pressure-limited ventilation while also guaranteeing adequate minute ventilation (Dojat, Brochard, Lemaire, & Harf, 1992; Laubscher, Heinrichs, Weiler, Hartmann, & Brunner, 1994; Sinderby et al., 1999; Younes et al., 1992). One of the major difficulties in designing an efficient control algorithm for mechanical ventilation is that the parameters characterising the dynamics of the lungs, that is, the lung resistances and lung compliances vary from patient to patient as well as within the same patient under different conditions. Another challenge is that the volume of each compartment cannot be directly measured and only the total volume of the lungs is available. Therefore, only partial state information can be used in the controller for feedback. With the advances in microchip and sensing technology, the total lung volume can be accurately measured by an electronic spirometer (Kramme, Hoffmann, & Pozos, 2011, chap. 8).

The spirometer detects the flow rate from the sensor and digitally integrates flow to volume. Various types of flow sensors such as diaphragm pneumotachometers, turbine flowmeters, vortex flowmeters, and ultrasound flowmeters are used in different spirometers. The ultrasound flowmeter offers high accuracy and is calibration-free (Kramme et al., 2011). One such spirometer that uses ultrasound flowmeter is EasyOne spirometer. Taking into account the unavailability of the state information and parameter uncertainties, an output feedback robust control methodology is needed in order to design an efficient control algorithm. A model predictive control for a multi-compartment respiratory system has been recently proposed in Li and Haddad (2013), whereas a neuroadaptive controller for mechanical ventilation was developed in Volyanskyy et al. (2011). Although parameter uncertainty was addressed in Volyanskyy et al. (2011), system disturbances were not addressed in either work.

Sliding mode control has been widely used in the literature due to its ability in handling system uncertainty and system disturbances (Edwards & Spurgeon, 1998; Slotine & Li, 1991; Utkin, 1977). An output feedback sliding mode controller for linear systems has been presented in Edwards and Spurgeon (1998). However, the results of Edwards and Spurgeon (1998) are only applicable to linear time-invariant systems since a system transformation is needed in order to transform the dynamical system into an appropriate form (see Edwards & Spurgeon, 1998, chap. 5). As shown in Chellaboina, Haddad, Li, and Bailey (2010), a respiratory system gives rise to a switched dynamical system since the values of the respiratory parameters – lung resistances and lung compliances – differ during the inspiration and expiration phases. For a switched (time-varying) system, a time-varying transformation is needed in employing the results of Edwards and Spurgeon (1998), and hence, the results in Edwards and Spurgeon (1998) are no longer valid. Further-

more, the respiratory system dynamics give rise to a nonnegative compartmental system, where, additionally, the input to the system is restricted to be nonnegative. Therefore, the method proposed in Edwards and Spurgeon (1998) cannot be directly applied to the respiratory model developed in Chellaboina et al. (2010). Although there exist numerous results on output feedback sliding mode control for dynamical systems (Edwards & Spurgeon, 1998; Nunes, Hsu, & Lizarralde, 2009; Zhang and Xia, 2010), sliding mode control for nonnegative dynamical system is nonexistent in the literature.

In this paper, we develop a sliding mode control architecture to control lung volume and minute ventilation in the presence of modelling uncertainties. Since the applied pressure is generally nonnegative and cannot be arbitrarily large, as not to cause lung injury, a sliding mode controller with bounded nonnegative control inputs is proposed. Unlike the neuroadaptive controller proposed in Volyanskyy et al. (2011), where an estimate of the full-state variables is required, our approach does not require full-state reconstruction information. Furthermore, unlike Edwards and Spurgeon (1998) and Zhang and Xia (2010), where a system transformation is employed to transform a linear time-invariant system into an appropriate form, such a system transformation cannot be applied in this paper since the respiratory system gives rise to a switched (i.e., time-varying) dynamical system. Our proposed control method first guarantees that the system states are bounded for a bounded control input. Then, a sliding mode controller is designed to track a given reference signal in the presence of system uncertainty and system disturbances. Moreover, standard uncertainty matching conditions (Edwards and Spurgeon, 1998; Nunes et al., 2009) that are required in sliding mode control formulations are relaxed. Specifically, we develop a control framework for both matched and unmatched parameter uncertainties. Finally, an illustrative numerical example is presented to demonstrate the efficacy of the proposed control framework.

2. Dynamics of respiratory system

2.1 Notation

For $x \in \mathbb{R}^n$, we write $x \geq 0$ (respectively, $x >> 0$) to indicate that every component x_i of x is nonnegative (respectively, positive). For $x, y \in \mathbb{R}^n$, we write $x \geq y$ to indicate that $x_i \geq y_i$, $i = 1, 2, \dots, n$. Furthermore, for $A \in \mathbb{R}^{n \times n}$, we write $A \geq 0$ (respectively, $A >> 0$) to indicate that every entry of A is nonnegative (respectively, positive) and $A \geq 0$ (respectively, $A > 0$) to indicate that A is nonnegative (respectively, positive) definite. Moreover, we write $\overline{\mathbb{R}}_+^n$ and \mathbb{R}_+^n to denote the nonnegative and positive orthants of \mathbb{R}^n , that is, if $x \in \mathbb{R}^n$, then $x \in \overline{\mathbb{R}}_+^n$ and $x \in \mathbb{R}_+^n$ are equivalent, respectively, to $x \geq 0$ and $x >> 0$. Finally, let $\mathbf{e}_n \in \mathbb{R}^n$ denote the one's vector of order n , that is, $\mathbf{e}_n = [1, 1, \dots, 1]^T$;

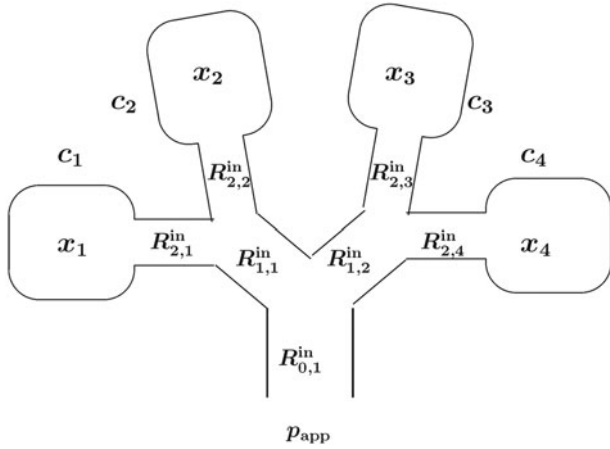


Figure 1. Four-compartment lung model.

if the order of e_n is clear from context we simply write e for e_n .

2.2 Multi-compartment respiratory system model

In this section, we present a general mathematical model for the dynamics of a multi-compartment respiratory system. We assume that the bronchial tree has a regular dichotomy structure, that is, in every generation each airway unit branches in two airway units of the subsequent generation (Chellaboina et al., 2010; Weibel, 1963). In this model, the lungs are represented as 2^n lung units which are connected to the pressure source by n generation of airway units, where each unit branches into two airways of the subsequent generation leading to 2^n compartments. A graphical illustration of a four-compartment lung model is shown in Figure 1.

Let $x_i, i = 1, 2, \dots, 2^n$, denote the lung volume in the i th compartment, let $c_i, i = 1, 2, \dots, 2^n$, denote the compliance of each compartment, and let $R_{j,i}^{in}$ (respectively, $R_{j,i}^{ex}$), $i = 1, 2, \dots, 2^j, j = 0, 1, \dots, n$, denote the resistance (to air flow) of the i th airway in the j th generation during inspiration (respectively, expiration) period with $R_{0,1}^{in}$ (respectively, $R_{0,1}^{ex}$) denoting the inspiration (respectively, expiration) of the parent (i.e., 0th generation) airway. The state equations for inspiration and expiration are given by Chellaboina et al. (2010):

$$R_{in}\dot{x}(t) + Cx(t) = p_{in}(t)e, \quad x(0) = x_0^{in}, \quad 0 \leq t \leq T_{in}, \quad (1)$$

$$R_{ex}\dot{x}(t) + Cx(t) = p_{ex}(t)e, \quad x(T_{in}) = x_0^{ex}, \quad T_{in} \leq t \leq T_{in} + T_{ex}, \quad (2)$$

where $x \triangleq [x_1, x_2, \dots, x_{2^n}]^T, C \triangleq \text{diag}[\frac{1}{c_1}, \dots, \frac{1}{c_{2^n}}], p_{in}(t), 0 \leq t \leq T_{in}$, and $p_{ex}(t), T_{in} \leq t \leq T_{ex}$, denote the input pressures during inspiration and expiration, respectively,

T_{in} and T_{ex} denote the duration of inspiration and expiration, respectively, and $R_{in} \triangleq \sum_{j=0}^n \sum_{k=1}^{2^j} R_{j,k}^{in} Z_{j,k} Z_{j,k}^T$ and $R_{ex} \triangleq \sum_{j=0}^n \sum_{k=1}^{2^j} R_{j,k}^{ex} Z_{j,k} Z_{j,k}^T$, where $Z_{j,k} \in \mathbb{R}^{2^n}$ is such that the l th component of $Z_{j,k}$ is 1 for all $l = (k-1)2^{n-j} + 1, (k-1)2^{n-j} + 2, \dots, k2^{n-j}, k = 1, \dots, 2^j, j = 0, 1, \dots, n$, and zero elsewhere.

Equations (1) and (2) can thus be written as

$$\dot{x}(t) = A_{in}x(t) + B_{in}p_{in}(t), \quad x(0) = x_0^{in}, \quad 0 \leq t \leq T_{in}, \quad (3)$$

$$\dot{x}(t) = A_{ex}x(t) + B_{ex}p_{ex}(t), \quad x(T_{in}) = x_0^{ex}, \quad T_{in} \leq t \leq T_{in} + T_{ex}, \quad (4)$$

where $A_{in} \triangleq -R_{in}^{-1}C, B_{in} \triangleq R_{in}^{-1}e, A_{ex} \triangleq -R_{ex}^{-1}C$, and $B_{ex} \triangleq R_{ex}^{-1}e$. The inspiration process is assumed to start from a given initial state x_0^{in} and followed by the expiration process. The initial value of the expiration process is the final value of the inspiration process. One complete inspiration and expiration process is called a *breathing cycle*. It is assumed that each breathing cycle is followed by another breathing cycle. Therefore, it is clear that the respiratory system given by Equations (3) and (4) is a periodic system with period $T = T_{in} + T_{ex}$.

Note that a linear system represented by Equations (3) and (4) is a switched linear system where the system parameters – the lung resistances and lung compliances – change between the inspiration and expiration phases. Hence, the dynamics for a breathing cycle can be characterised by the periodic switched dynamical system given by

$$\dot{x}(t) = A(t)x(t) + B(t)u(t), \quad x(0) = x_0^{in}, \quad t \geq 0, \quad (5)$$

where

$$A(t) = A(t + T), \quad t \geq 0, \quad (6)$$

$$A(t) = \begin{cases} A_{in}, & 0 \leq t < T_{in}, \\ A_{ex}, & T_{in} \leq t < T, \end{cases} \quad (7)$$

$$B(t) = \begin{cases} B_{in}, & 0 \leq t < T_{in}, \\ B_{ex}, & T_{in} \leq t < T, \end{cases} \quad (8)$$

$$u(t) = \begin{cases} u^{in}(t), & 0 \leq t < T_{in}, \\ u^{ex}(t), & T_{in} \leq t < T. \end{cases} \quad (9)$$

The solution to Equation (5) over the time interval $[0, T]$ is given by (Chellaboina et al., 2010):

$$x(t) = \begin{cases} e^{A_{in}t}x_0^{in} + \int_0^t e^{A_{in}(t-\tau)}B_{in}u_1^{in}(\tau)d\tau, & 0 \leq t \leq T_{in}, \\ e^{A_{ex}(t-T_{in})}x_0^{ex} + \int_{T_{in}}^t e^{A_{ex}(t-\tau)}B_{ex}u_1^{ex}(\tau)d\tau, & T_{in} \leq t \leq T, \end{cases} \quad (10)$$

where $x_1^{\text{in}}(t), t \in [0, T_{\text{in}}]$, and $u_1^{\text{ex}}(t), t \in [T_{\text{in}}, T]$, are the inspiration and expiration input pressures, respectively, during the first breathing cycle.

It follows from Equation (10) that

$$x_0^{\text{ex}} = x(T_{\text{in}}) = \Gamma_{\text{in}} x_0^{\text{in}} + \theta_1, \tag{11}$$

where $\Gamma_{\text{in}} \triangleq e^{A_{\text{in}} T_{\text{in}}}$ and $\theta_1 \triangleq e^{A_{\text{in}} T_{\text{in}}} \int_0^{T_{\text{in}}} e^{-A_{\text{in}} t} B_{\text{in}} u_1^{\text{in}}(t) dt$. Furthermore, note that

$$x(T) = \Gamma_{\text{ex}} x_0^{\text{ex}} + \delta_1, \tag{12}$$

where $\Gamma_{\text{ex}} \triangleq e^{A_{\text{ex}} T_{\text{ex}}}$ and $\delta_1 \triangleq e^{A_{\text{ex}} T} \int_{T_{\text{in}}}^T e^{-A_{\text{ex}} t} B_{\text{ex}} u_1^{\text{ex}}(t) dt$.

Next, let x_m^{in} and $u_m^{\text{in}}(t), t \in [0, T_{\text{in}}]$, denote, respectively, the initial condition and input pressure for the m th inspiration, and let x_m^{ex} and $u_m^{\text{ex}}(t), t \in [T_{\text{in}}, T]$, denote, respectively, the initial condition and input pressure for the m th expiration, that is, $x_m^{\text{in}} = x(mT)$ and $x_m^{\text{ex}} = x(mT + T_{\text{in}})$, $m = 0, 1, \dots$. Hence, it follows from Equations (11) and (12) that

$$x_1^{\text{in}} = \Gamma_{\text{ei}} x_0^{\text{in}} + \Gamma_{\text{ex}} \theta_1 + \delta_1, \tag{13}$$

$$x_1^{\text{ex}} = \Gamma_{\text{ie}} x_0^{\text{ex}} + \Gamma_{\text{in}} \delta_1 + \theta_1, \tag{14}$$

where $\Gamma_{\text{ei}} \triangleq \Gamma_{\text{ex}} \Gamma_{\text{in}}$ and $\Gamma_{\text{ie}} \triangleq \Gamma_{\text{in}} \Gamma_{\text{ex}}$. More generally,

$$x_{m+1}^{\text{in}} = \Gamma_{\text{ei}} x_m^{\text{in}} + \Gamma_{\text{ex}} \theta_{m+1} + \delta_{m+1}, \quad m = 0, 1, \dots, \tag{15}$$

$$x_{m+1}^{\text{ex}} = \Gamma_{\text{ie}} x_m^{\text{ex}} + \Gamma_{\text{in}} \delta_{m+1} + \theta_{m+1}, \quad m = 0, 1, \dots, \tag{16}$$

where

$$\delta_{m+1} \triangleq e^{A_{\text{ex}} T} \int_{T_{\text{in}}}^T e^{-A_{\text{ex}} t} B_{\text{ex}} u_{m+1}^{\text{ex}}(t) dt, \tag{17}$$

$$\theta_{m+1} \triangleq e^{A_{\text{in}} T_{\text{in}}} \int_0^{T_{\text{in}}} e^{-A_{\text{in}} t} B_{\text{in}} u_{m+1}^{\text{in}}(t) dt. \tag{18}$$

Now, Equations (15) and (16) can be, respectively, written as

$$x_m^{\text{in}} = \Gamma_{\text{ei}}^m x_0^{\text{in}} + \sum_{j=0}^{m-1} \Gamma_{\text{ei}}^j (\Gamma_{\text{ex}} \theta_{m-j} + \delta_{m-j}), \quad m = 0, 1, \dots, \tag{19}$$

$$x_m^{\text{ex}} = \Gamma_{\text{ie}}^m x_0^{\text{ex}} + \sum_{j=0}^{m-1} \Gamma_{\text{ie}}^j (\Gamma_{\text{in}} \delta_{m-j} + \theta_{m-j}), \quad m = 0, 1, \dots. \tag{20}$$

The following definition and lemmas are needed for the main results of the paper.

Definition 2.1 (Chellaboina et al., 2010): Let $A \in \mathbb{R}^{n \times n}$. A is *essentially nonnegative* if $A_{i,j} \geq 0, i, j = 1, \dots, n, i \neq j$. A is *compartmental* if A is essentially nonnegative and $A^T \mathbf{e} \leq 0$.

Lemma 2.1 (Chellaboina et al., 2010): A_{in} and A_{ex} are *compartmental and Hurwitz*, $e^{A_{\text{in}} t} \geq 0$ and $e^{A_{\text{ex}} t} \geq 0$ for all $t \geq 0$, and $B_{\text{in}} \geq 0$ and $B_{\text{ex}} \geq 0$.

Lemma 2.2 (Chellaboina et al., 2010): Γ_{ie} and Γ_{ei} are *Schur*, and hence, $\lim_{m \rightarrow \infty} \Gamma_{\text{ie}}^m = 0$ and $\lim_{m \rightarrow \infty} \Gamma_{\text{ei}}^m = 0$. Furthermore, $(I - \Gamma_{\text{ei}})^{-1}$ and $(I - \Gamma_{\text{ie}})^{-1}$ exist and are given by $(I - \Gamma_{\text{ei}})^{-1} = \sum_{j=0}^{\infty} \Gamma_{\text{ei}}^j$ and $(I - \Gamma_{\text{ie}})^{-1} = \sum_{j=0}^{\infty} \Gamma_{\text{ie}}^j$.

Proposition 2.1: Consider the switched dynamical system given by Equation (5). If $|u(t)| \leq u^*, t \geq 0$, where u^* is a positive constant, then $x(t)$ is bounded for all $t \geq 0$.

Proof: Let $\theta_{\text{max}} \triangleq e^{A_{\text{in}} T_{\text{in}}} \int_0^{T_{\text{in}}} e^{-A_{\text{in}} t} B_{\text{in}} u^* dt$ and $\delta_{\text{max}} \triangleq e^{A_{\text{ex}} T} \int_{T_{\text{in}}}^T e^{-A_{\text{ex}} t} B_{\text{ex}} u^* dt$. It follows from Lemma 2.1 that $-\theta_{\text{max}} \leq \theta_m \leq \theta_{\text{max}}$ and $-\delta_{\text{max}} \leq \delta_m \leq \delta_{\text{max}}, m = 1, 2, \dots$. Hence, using Equations (19) and (20), it follows that

$$\hat{x}_m^{\text{in}} \leq x_m^{\text{in}} \leq \bar{x}_m^{\text{in}}, \quad m = 1, 2, \dots, \tag{21}$$

$$\hat{x}_m^{\text{ex}} \leq x_m^{\text{ex}} \leq \bar{x}_m^{\text{ex}}, \quad m = 1, 2, \dots, \tag{22}$$

where $\hat{x}_m^{\text{in}} \triangleq \Gamma_{\text{ei}}^m \hat{x}_0^{\text{in}} - \sum_{j=0}^{m-1} \Gamma_{\text{ei}}^j (\Gamma_{\text{ex}} \theta_{\text{max}} + \delta_{\text{max}})$, $\bar{x}_m^{\text{in}} \triangleq \Gamma_{\text{ei}}^m \bar{x}_0^{\text{in}} + \sum_{j=0}^{m-1} \Gamma_{\text{ei}}^j (\Gamma_{\text{ex}} \theta_{\text{max}} + \delta_{\text{max}})$, $\hat{x}_m^{\text{ex}} \triangleq \Gamma_{\text{ie}}^m \hat{x}_0^{\text{ex}} - \sum_{j=0}^{m-1} \Gamma_{\text{ie}}^j (\Gamma_{\text{in}} \delta_{\text{max}} + \theta_{\text{max}})$, and $\bar{x}_m^{\text{ex}} \triangleq \Gamma_{\text{ie}}^m \bar{x}_0^{\text{ex}} + \sum_{j=0}^{m-1} \Gamma_{\text{ie}}^j (\Gamma_{\text{in}} \delta_{\text{max}} + \theta_{\text{max}})$. In addition, note that $\hat{x}_0^{\text{in}} = \bar{x}_0^{\text{in}} = x_0^{\text{in}}$, $\hat{x}_0^{\text{ex}} = \Gamma_{\text{in}} x_0^{\text{in}} - \theta_{\text{max}}$, and $\bar{x}_0^{\text{ex}} = \Gamma_{\text{in}} x_0^{\text{in}} + \theta_{\text{max}}$.

Next, note that the solution to Equation (5) for the m th period is given by

$$x(t + (m-1)T) = \begin{cases} e^{A_{\text{in}} t} x_{m-1}^{\text{in}} + \int_0^t e^{A_{\text{in}}(t-\tau)} B_{\text{in}} u_m^{\text{in}}(\tau) d\tau, & 0 \leq t \leq T_{\text{in}}, \\ e^{A_{\text{ex}}(t-T_{\text{in}})} x_{m-1}^{\text{ex}} + \int_{T_{\text{in}}}^t e^{A_{\text{ex}}(t-\tau)} B_{\text{ex}} u_m^{\text{ex}}(\tau) d\tau, & T_{\text{in}} \leq t \leq T. \end{cases}$$

Since $\hat{x}_{m-1}^{\text{in}} \leq x_{m-1}^{\text{in}} \leq \bar{x}_{m-1}^{\text{in}}, |u_m^{\text{in}}(t)| \leq u^*, t \in [0, T_{\text{in}}]$, $\hat{x}_{m-1}^{\text{ex}} \leq x_{m-1}^{\text{ex}} \leq \bar{x}_{m-1}^{\text{ex}}$, and $|u_m^{\text{ex}}(t)| \leq u^*, t \in [T_{\text{in}}, T]$, it follows that

$$\hat{x}(t + (m-1)T) \leq x(t + (m-1)T) \leq \bar{x}(t + (m-1)T), \quad 0 \leq t \leq T, \tag{23}$$

where

$$\hat{x}(t + (m-1)T) = \begin{cases} e^{A_{\text{in}} t} \hat{x}_{m-1}^{\text{in}} - \int_0^t e^{A_{\text{in}}(t-\tau)} B_{\text{in}} u^* d\tau, & 0 \leq t \leq T_{\text{in}}, \\ e^{A_{\text{ex}}(t-T_{\text{in}})} \hat{x}_{m-1}^{\text{ex}} - \int_{T_{\text{in}}}^t e^{A_{\text{ex}}(t-\tau)} B_{\text{ex}} u^* d\tau, & T_{\text{in}} \leq t \leq T, \end{cases} \tag{24}$$

and

$$\begin{aligned} & \bar{x}(t + (m-1)T) \\ &= \begin{cases} e^{A_{in}t} \bar{x}_{m-1}^{in} + \int_0^t e^{A_{in}(t-\tau)} B_{in} u^* d\tau, & 0 \leq t \leq T_{in}, \\ e^{A_{ex}(t-T_{in})} \bar{x}_{m-1}^{ex} + \int_{T_{in}}^t e^{A_{ex}(t-\tau)} B_{ex} u^* d\tau, & T_{in} \leq t \leq T. \end{cases} \end{aligned} \quad (25)$$

Now, since $\hat{x}_m^{in} = \Gamma_{ei}^m \hat{x}_0^{in} - \sum_{j=0}^{m-1} \Gamma_{ei}^j (\Gamma_{ex} \theta_{max} + \delta_{max})$ and $\hat{x}_m^{ex} = \Gamma_{ie}^m \hat{x}_0^{ex} - \sum_{j=0}^{m-1} \Gamma_{ie}^j (\Gamma_{in} \delta_{max} + \theta_{max})$, it follows from Lemma 2.2 that $\lim_{m \rightarrow \infty} \hat{x}_m^{in} = -(I - \Gamma_{ei})^{-1} (\Gamma_{ex} \theta_{max} + \delta_{max})$ and $\lim_{m \rightarrow \infty} \hat{x}_m^{ex} = -(I - \Gamma_{ie})^{-1} (\Gamma_{in} \delta_{max} + \theta_{max})$. Thus, it follows from Equation (24) that for $\hat{x}_0^{in} = x_0^{in}$, $\hat{x}(t + (m-1)T)$, $0 \leq t \leq T$, $m = 1, 2, \dots$, is finite, and hence, $\hat{x}(t)$ is bounded for all $t \geq 0$. Similarly, $\bar{x}(t)$ is bounded for all $t \geq 0$. Furthermore, Equation (23) implies that $x(t + (m-1)T)$, $0 \leq t \leq T$, $m = 1, 2, \dots$, is bounded or, equivalently, $x(t)$ is bounded for all $t \geq 0$. \square

Remark 2.1: The values of θ_{max} and δ_{max} can be computed as

$$\begin{aligned} \theta_{max} &= e^{A_{in}T_{in}} \int_0^{T_{in}} e^{-A_{in}t} B_{in} u^* dt \\ &= A_{in}^{-1} \left(-e^{-A_{in}(t-T_{in})} \Big|_0^{T_{in}} \right) B_{in} u^* \\ &= A_{in}^{-1} (e^{A_{in}T_{in}} - I) B_{in} u^* \end{aligned} \quad (26)$$

and, similarly,

$$\delta_{max} = A_{ex}^{-1} (e^{A_{ex}T_{ex}} - I) B_{ex} u^*. \quad (27)$$

Furthermore, note that if $u(t) = 0$ for all $t \geq 0$, then $\lim_{m \rightarrow \infty} \hat{x}_m^{in} = \lim_{m \rightarrow \infty} \hat{x}_m^{ex} = \lim_{m \rightarrow \infty} \bar{x}_m^{in} = \lim_{m \rightarrow \infty} \bar{x}_m^{ex} = 0$, and hence, $x(t) \rightarrow 0$ as $t \rightarrow \infty$.

3. Sliding mode control problem formulation

In this section, we present an output feedback sliding mode control architecture for trajectory tracking for the respiratory system developed in Section 2. Specifically, consider the switched linear nonnegative uncertain dynamical system \mathcal{G} given by

$$\begin{aligned} \dot{x}(t) &= A(t)x(t) + B(t)[h(u(t)) + d(t)], \\ x(0) &= x_0^{in}, \quad t \geq 0, \end{aligned} \quad (28)$$

$$y(t) = e^T x(t), \quad (29)$$

where $x(t) \in \mathbb{R}^{2n}$, $t \geq 0$, is the state vector, $u(t) \in \mathbb{R}$, $t \geq 0$, is the control input, $y(t) \in \mathbb{R}$, $t \geq 0$, is the system output, and $h(u(t))$, $t \geq 0$, is the constraint control input given by

$$h(u(t)) \triangleq \begin{cases} 0, & u(t) \leq 0, \\ u(t), & 0 \leq u(t) \leq u_{max}, \\ u_{max}, & u(t) \geq u_{max}, \end{cases} \quad (30)$$

where $u_{max} > 0$ is a given constant, $d(t) \in \mathbb{R}$, $t \geq 0$, is a bounded system disturbance representing the disturbance generated by the mechanical ventilator and is such that $|d(t)| \leq d^*$, where d^* is a positive constant, $A(t) \in \mathbb{R}^{2n \times 2n}$, $t \geq 0$, and $B(t) \in \mathbb{R}^{2n}$, $t \geq 0$, are given by Equations (7) and (8), respectively.

Next, let $A(t) = \hat{A}(t) + \Delta A(t)$ and $B(t) = \hat{B}(t) + \Delta B(t)$, where $\hat{A}(t) \in \mathbb{R}^{2n \times 2n}$, $t \geq 0$, is the nominal value of $A(t)$, $\Delta A(t) \in \mathbb{R}^{2n \times 2n}$, $t \geq 0$, is the uncertainty in $A(t)$, $\hat{B}(t) \in \mathbb{R}^{2n}$, $t \geq 0$, is the nominal value of $B(t)$, and $\Delta B(t) \in \mathbb{R}^{2n}$, $t \geq 0$, is the uncertainty in $B(t)$. The uncertainties $\Delta A(t)$, $t \geq 0$, and $\Delta B(t)$, $t \geq 0$, are assumed to be unknown but bounded by some known constant matrices. Specifically, we assume $\|\Delta A(t)\| \leq \|A^*\|$, $t \geq 0$, and $\|\Delta B(t)\| \leq \|B^*\|$, $t \geq 0$, where $A^* \in \mathbb{R}^{2n \times 2n}$ and $B^* \in \mathbb{R}^{2n}$ are known matrices. Furthermore, we assume that $\hat{B}(t)$, $t \geq 0$, is nonnegative and $\text{rank } \hat{B}(t) \neq 0$, $t \geq 0$.

In order to achieve output tracking, we construct a reference nonnegative dynamical system \mathcal{G}_r given by

$$\dot{x}_r(t) = A_r(t)x_r(t) + B_r(t)r(t), \quad x_r(0) = x_{r0}, \quad t \geq 0, \quad (31)$$

$$y_r(t) = e^T x_r(t), \quad (32)$$

where $x_r(t) \in \mathbb{R}^{2n}$, $t \geq 0$, is the reference state vector, $r(t) \in \mathbb{R}$, $t \geq 0$, is a bounded piecewise continuous nonnegative reference input, $y_r(t) \in \mathbb{R}$, $t \geq 0$, is a reference output, $B_r(t) \in \mathbb{R}^{2n}$, $t \geq 0$, is a nonnegative matrix function, and $A_r(t) \in \mathbb{R}^{2n \times 2n}$, $t \geq 0$, is given by

$$A_r(t) = \begin{cases} A_{rin}, & 0 \leq t \leq T_{in}, \\ A_{rex}, & T_{in} \leq t \leq T_{ex}, \end{cases}$$

where $A_{rin} \in \mathbb{R}^{2n \times 2n}$ and $A_{rex} \in \mathbb{R}^{2n \times 2n}$ are compartmental and Hurwitz.

Assumption 3.1: There exist $k_y \in \mathbb{R}$ and $k_r \in \mathbb{R}$ such that

$$A_r(t) = \hat{A}(t) + k_y \hat{B}(t) e^T \quad (33)$$

and

$$B_r(t) = k_r \hat{B}(t). \quad (34)$$

Assumption 3.1 involves a standard matching condition for model reference adaptive control appearing in the literature (see, for example, Tao, 2003, chap. 5). The assumption ensures that the system is able to follow the reference model perfectly. Specifically, for our system, Assumption 3.1 implies that the reference system is chosen in such a way so that the lung mechanics system is capable of following the reference model perfectly if there is no restriction on the input pressure.

Next, defining $f : \mathbb{R}^{2n} \times \bar{\mathbb{R}}_+ \times \mathbb{R} \rightarrow \mathbb{R}^{2n}$ by $f(x(t), h(u(t)), d(t)) \triangleq \Delta A(t)x(t) + \Delta B(t)h(u(t)) + B(t)d(t)$, the

dynamics in Equation (28) can be written as

$$\dot{x}(t) = \hat{A}(t)x(t) + \hat{B}(t)h(u(t)) + f(x(t), h(u(t)), d(t)),$$

$$x(0) = x_0^{\text{in}}, \quad t \geq 0. \quad (35)$$

Now, consider the control input $u(t)$, $t \geq 0$, given by

$$u(t) = u_f(t) + u_s(t), \quad (36)$$

where

$$u_f(t) = k_y y(t) + k_r r(t), \quad (37)$$

and $u_s(t) \in \mathbb{R}$, $t \geq 0$, is a sliding mode controller to be defined later. Next, defining the tracking error state $e(t) \triangleq x(t) - x_r(t)$, $t \geq 0$, and using Equations (36), (37), and Assumption 3.1, the error dynamics are given by

$$\dot{e}(t) = A_r(t)e(t) + \hat{B}(t)u_s(t) + \hat{B}(t)\Delta h(u(t)) + f(x(t), h(u(t)), d(t)), \quad e(0) = x_0^{\text{in}} - x_{r0}, \quad t \geq 0, \quad (38)$$

where $\Delta h(u(t)) \triangleq h(u(t)) - u(t)$, $t \geq 0$.

To account for the effects of control saturation (pressure-limited respiration) on the error state $e(t)$, $t \geq 0$, consider the dynamical system given by (Volyanskyy et al., 2011):

$$\dot{e}_s(t) = A_r(t)e_s(t) + \hat{B}(t)\Delta h(u(t)), \quad e_s(0) = e_{s0}, \quad t \geq 0, \quad (39)$$

$$y_s(t) = \mathbf{e}^T e_s(t), \quad (40)$$

where $e_s(t) \in \mathbb{R}^{2^n}$, $t \geq 0$, and define the shifted error state $\tilde{e}(t) \triangleq e(t) - e_s(t)$, $t \geq 0$. It follows from Equations (38) and (39) that

$$\dot{\tilde{e}}(t) = A_r(t)\tilde{e}(t) + f(x(t), h(u(t)), d(t)) + \hat{B}(t)u_s(t),$$

$$\tilde{e}(0) = \tilde{e}_0, \quad t \geq 0. \quad (41)$$

Now, define the switching function

$$s(\tilde{e}(t)) \triangleq y(t) - y_r(t) - y_s(t) = \mathbf{e}^T \tilde{e}(t), \quad (42)$$

and note that it follows from Equations (41) and (42) that

$$\dot{s}(\tilde{e}(t)) = \mathbf{e}^T \dot{\tilde{e}}(t) = \mathbf{e}^T A_r(t)\tilde{e}(t) + \mathbf{e}^T f(x(t), h(u(t)), d(t)) + \mathbf{e}^T \hat{B}(t)u_s(t), \quad s(0) = 0, \quad t \geq 0. \quad (43)$$

3.1 Output feedback sliding mode control with matched uncertainty

In this section, an output feedback sliding mode control with matched uncertainty is developed. Specifically, the

unknown function $f : \mathbb{R}^{2^n} \times \overline{\mathbb{R}}_+ \times \mathbb{R} \rightarrow \mathbb{R}^{2^n}$, which represents system uncertainty and system disturbances, is assumed to satisfy the matching condition (Edwards & Spurgeon, 1998) given by

$$f(x(t), h(u(t)), d(t)) = \hat{B}(t)\psi(x(t), h(u(t))) + B(t)d(t),$$

$$(x, h(u), d) \in \mathbb{R}^{2^n} \times \overline{\mathbb{R}}_+ \times \mathbb{R}, \quad (44)$$

where the bounded function $\psi : \mathbb{R}^{2^n} \times \overline{\mathbb{R}}_+ \rightarrow \mathbb{R}$ satisfies

$$|\psi(x(t), h(u(t)))| < kh(u(t)) + \alpha(y(t)),$$

$$(x, h(u)) \in \mathbb{R}^{2^n} \times \overline{\mathbb{R}}_+, \quad (45)$$

for some known function $\alpha : \mathbb{R} \rightarrow \mathbb{R}_+$ and positive constant $k \in (0, 1)$.

A controller $u_s(t)$, $t \geq 0$, is constructed as

$$u_s(t) = -(\mathbf{e}^T \hat{B}(t))^{-1} \rho(y(t), x_r(t), e_s(t)) \text{sgn}(s(\tilde{e}(t))), \quad (46)$$

where $\text{sgn}(s) \triangleq s/|s|$ for $s \neq 0$ and $\text{sgn}(0) \triangleq 0$, and $\rho(y(t), x_r(t), e_s(t))$, $t \geq 0$, is a positive scalar function given by

$$\rho(y(t), x_r(t), e_s(t)) = \frac{\gamma(y(t), x_r(t), e_s(t)) + \mathbf{e}^T \hat{B}(t)\alpha(y(t))}{1 - k}, \quad (47)$$

where $\gamma(y(t), x_r(t), e_s(t))$, $t \geq 0$, is a positive scalar function. Note that since $\hat{B}(t) \geq 0$ and $\text{rank } \hat{B}(t) \neq 0$ for all $t \geq 0$, it follows that $\mathbf{e}^T \hat{B}(t) > 0$, $t \geq 0$, and hence, $(\mathbf{e}^T \hat{B}(t))^{-1}$, $t \geq 0$, is well defined.

Theorem 3.1: Consider the switched linear uncertain dynamical system \mathcal{G} given by Equations (28) and (29) with $u(t)$, $t \geq 0$, given by Equations (36), (37), and (46), and reference model \mathcal{G}_r given by Equations (31) and (32). Assume that the matching conditions (33) and (34) and the uncertainty matching conditions (44) and (45) hold. Then, there exists a bounded positive function $\mu_1(y(t), x_r(t), e_s(t))$, $t \geq 0$, such that

$$\mu_1(y(t), x_r(t), e_s(t)) \geq |\mathbf{e}^T A_r(t)\tilde{e}(t)| + \mathbf{e}^T \hat{B}(t)k|u_f(t)| + \mathbf{e}^T B(t)d^*, \quad t \geq 0, \quad (48)$$

and, for $\gamma(y(t), x_r(t), e_s(t)) = \mu_1(y(t), x_r(t), e_s(t)) + \kappa_1$, $t \geq 0$, where κ_1 is a positive constant, the zero solution $s(\tilde{e}(t)) \equiv 0$ to the closed-loop system (43) is uniformly finite-time stable and $y(t) - y_r(t) \rightarrow y_s(t)$ in finite time.

Proof: Consider the Lyapunov function candidate

$$V(s(\tilde{e})) = \frac{1}{2}s^2(\tilde{e}) \quad (49)$$

and note that $V(0) = 0$ and $V(s(\tilde{e})) > 0$ for all $s(\tilde{e}) \neq 0$. Now, using Equations (43), (45), and (46), it follows that

the derivative of $V(s(\tilde{e}))$ along the closed-loop system trajectories of \mathcal{G} is given by

$$\begin{aligned}\dot{V}(s(\tilde{e}(t))) &= s(\tilde{e}(t))\dot{s}(\tilde{e}(t)) = s(\tilde{e}(t))[\mathbf{e}^T A_r(t)\tilde{e}(t) \\ &\quad + \mathbf{e}^T (\hat{B}(t)\psi(x(t), h(u(t))) + B(t)d(t)) \\ &\quad - \rho(y(t), x_r(t), e_s(t)) \operatorname{sgn}(s(\tilde{e}(t)))], \\ &\leq |s(\tilde{e}(t))| [|\mathbf{e}^T A_r(t)\tilde{e}(t)| + \mathbf{e}^T \hat{B}(t)(kh(u(t)) \\ &\quad + \alpha(y(t))) + \mathbf{e}^T B(t)|d(t)| \\ &\quad - \rho(y(t), x_r(t), e_s(t))], \quad t \geq 0. \quad (50)\end{aligned}$$

Next, note that it follows from Equations (30) and (36) that $h(u(t)) \leq |u(t)| \leq |u_f(t)| + |u_s(t)|$, $t \geq 0$. Now, since $|d(t)| < d^*$, $t \geq 0$, it follows from Equation (50) that

$$\begin{aligned}\dot{V}(s(\tilde{e}(t))) &\leq |s(\tilde{e}(t))| [|\mathbf{e}^T A_r(t)\tilde{e}(t)| + \mathbf{e}^T B(t)d^* \\ &\quad + \mathbf{e}^T \hat{B}(t)(k(|u_f(t)| + |u_s(t)|) + \alpha(y(t))) \\ &\quad - \rho(y(t), x_r(t), e_s(t))], \quad t \geq 0. \quad (51)\end{aligned}$$

In addition, it follows from Equation (46) that

$$|u_s(t)| = |(\mathbf{e}^T \hat{B}(t))^{-1} \rho(y(t), x_r(t), e_s(t)) \operatorname{sgn}(s(\tilde{e}(t)))|, \quad t \geq 0. \quad (52)$$

Since $\mathbf{e}^T \hat{B}(t) > 0$, $t \geq 0$, and $\rho(y(t), x_r(t), e_s(t)) > 0$, $t \geq 0$, it follows that

$$\begin{aligned}|u_s(t)| &= (\mathbf{e}^T \hat{B}(t))^{-1} \rho(y(t), x_r(t), e_s(t)) |\operatorname{sgn}(s(\tilde{e}(t)))| \\ &= (\mathbf{e}^T \hat{B}(t))^{-1} \rho(y(t), x_r(t), e_s(t)), \quad t \geq 0, \quad (53)\end{aligned}$$

and hence, it follows from Equation (47) that

$$\begin{aligned}\rho(y(t), x_r(t), e_s(t)) &= \gamma(y(t), x_r(t), e_s(t)) + \mathbf{e}^T \hat{B}(t)\alpha(y(t)) \\ &\quad + k\rho(y(t), x_r(t), e_s(t)) \\ &= \gamma(y(t), x_r(t), e_s(t)) + \mathbf{e}^T \hat{B}(t)(\alpha(y(t)) \\ &\quad + k|u_s(t)|), \quad t \geq 0. \quad (54)\end{aligned}$$

Therefore, it follows from Equations (51) and (54) that

$$\begin{aligned}\dot{V}(s(\tilde{e}(t))) &\leq |s(\tilde{e}(t))| [|\mathbf{e}^T A_r(t)\tilde{e}(t)| + \mathbf{e}^T B(t)d^* \\ &\quad + \mathbf{e}^T \hat{B}(t)k|u_f(t)| - \gamma(y(t), x_r(t), e_s(t))], \\ &\quad t \geq 0. \quad (55)\end{aligned}$$

Next, note that $y(t) = \mathbf{e}^T x(t) = x_1(t) + x_2(t) + \cdots + x_{2^n}(t)$, $t \geq 0$. Now, since the volume of each compartment is nonnegative, $x_1(t) + x_2(t) + \cdots + x_{2^n}(t) \geq \sqrt{x_1^2(t) + x_2^2(t) + \cdots + x_{2^n}^2(t)}$, $t \geq 0$, and hence, $\|x(t)\| \leq y(t)$, $t \geq 0$, where $\|\cdot\|$ denotes the Euclidean norm. Moreover, since $h(u(t))$, $t \geq 0$, and $d(t)$, $t \geq 0$, are bounded, it

follows from Proposition 2.1 and Equation (28) that $x(t)$, $t \geq 0$, is bounded, and hence, $y(t)$, $t \geq 0$, is bounded. From Proposition 2.1 and Equation (39), it follows that $e_s(t)$, $t \geq 0$, is bounded, and hence, we can choose a bounded positive function $\mu_1(y(t), x_r(t), e_s(t))$, $t \geq 0$, such that

$$\begin{aligned}\mu_1(y(t), x_r(t), e_s(t)) &= \|\mathbf{e}^T A_r(t)\| (y(t) + \|x_r(t)\| + \|e_s(t)\|) \\ &\quad + \mathbf{e}^T \hat{B}(t)k(|k_y y(t)| + |k_r r_{\max}|) \\ &\quad + (|\mathbf{e}^T \hat{B}(t)| + \|\mathbf{e}^T\| \|B^*\|)d^* \\ &\geq \|\mathbf{e}^T A_r(t)\| (\|x(t)\| + \|x_r(t)\| \\ &\quad + \|e_s(t)\|) + \mathbf{e}^T \hat{B}(t)k|k_y y(t) \\ &\quad + k_r r(t)| + (|\mathbf{e}^T \hat{B}(t)| \\ &\quad + \|\mathbf{e}^T\| \|\Delta B(t)\|)d^* \\ &\geq \|\mathbf{e}^T A_r(t)\| \|\tilde{e}(t)\| + \mathbf{e}^T \hat{B}(t)k|k_y y(t) \\ &\quad + k_r r(t)| + (|\mathbf{e}^T \hat{B}(t)| + |\mathbf{e}^T \Delta B(t)|)d^* \\ &\geq |\mathbf{e}^T A_r(t)\tilde{e}(t)| + \mathbf{e}^T \hat{B}(t)k|u_f(t)| \\ &\quad + \mathbf{e}^T B(t)d^*, \quad t \geq 0, \quad (56)\end{aligned}$$

where r_{\max} is the maximum input pressure to the reference model. Thus, $\mu_1(y(t), x_r(t), e_s(t))$, $t \geq 0$, satisfies Equation (48).

Finally, it follows from Equations (55) and (56) that

$$\begin{aligned}\dot{V}(s(\tilde{e}(t))) &\leq -(\gamma(y(t), x_r(t), e_s(t)) \\ &\quad - \mu_1(y(t), x_r(t), e_s(t)))|s(\tilde{e}(t))| \\ &= -\sqrt{2}(\gamma(y(t), x_r(t), e_s(t)) \\ &\quad - \mu_1(y(t), x_r(t), e_s(t))) (V(s(\tilde{e}(t))))^{\frac{1}{2}}, \\ &\quad t \geq 0, \quad (57)\end{aligned}$$

and for $\gamma(y(t), x_r(t), e_s(t)) = \mu_1(y(t), x_r(t), e_s(t)) + \kappa_1$, $t \geq 0$,

$$\dot{V}(s(\tilde{e}(t))) \leq -\sqrt{2}\kappa_1 (V(s(\tilde{e}(t))))^{\frac{1}{2}}, \quad t \geq 0. \quad (58)$$

Thus, it follows from Theorem 13.2 of Haddad, Nersesov, and Du (2009, p. 144) that the zero solution $s(\tilde{e}(t)) \equiv 0$ to the closed-loop system (43) with control input given by Equations (36), (37), and (46) is uniformly finite-time stable, and hence, $y(t) - y_r(t) \rightarrow y_s(t)$ in finite time. \square

Remark 3.1: If the control input $u(t)$, $t \geq 0$, is within the allowable range, that is, $u(t) \in [0, u_{\max}]$, $t \geq 0$, then $\Delta h(u(t)) = 0$, $t \geq 0$. In this case, it follows from Remark 2.1 and Equation (39) that $e_s(t)$, $t \geq 0$, converges to zero, and hence, $y_s(t)$, $t \geq 0$, converges to zero. Therefore, $y(t) - y_r(t)$, $t \geq 0$, converges to zero. However, when the control input $u(t)$, $t \geq 0$, is not within the allowable range, that is, $u(t) \notin [0, u_{\max}]$, $t \geq 0$, then $\Delta h(u(t)) \neq 0$, $t \geq 0$, and $y(t) - y_r(t) \rightarrow y_s(t)$, where $y_s(t)$, $t \geq 0$, is bounded.

Remark 3.2: Note that Theorem 3.1 guarantees that the total lung volume converges to the reference output $y_r(t)$, $t \geq 0$. In addition, Theorem 3.1 shows that the individual compartmental lung volumes, $x_i(t)$, $i = 1, 2, \dots, 2^n$, $t \geq 0$, are bounded for a bounded control input. However, since the control input is not necessarily periodic, it is not possible to show the convergence of the individual compartmental lung volumes to the state values of the reference model. If the control input is periodic, then the individual compartmental lung volumes for a pressure-limited respiratory system converge to steady-state end-inspiratory and end-expiratory values.

3.2 Output feedback sliding mode control with unmatched uncertainty

The matching condition in Equation (44), which appears in the output feedback sliding mode control literature (see, for example, Edwards & Spurgeon, 1998), can be restrictive. In this section, we develop an output feedback sliding mode controller where the uncertainty matching condition in Equation (44) is relaxed. Specifically, the controller $u_s(t)$, $t \geq 0$, is constructed as

$$u_s(t) = -(\mathbf{e}^T \hat{B}(t))^{-1} \beta(y(t), x_r(t), e_s(t)) \operatorname{sgn}(s(\tilde{e}(t))), \quad (59)$$

where $\beta(y(t), x_r(t), e_s(t))$, $t \geq 0$, is a positive function.

Theorem 3.2: Consider the switched linear uncertain dynamical system \mathcal{G} given by Equations (28) and (29) with $u(t)$, $t \geq 0$, given by Equations (36), (37), and (59), and reference model \mathcal{G}_r given by Equations (31) and (32). Assume that the matching conditions (33) and (34) hold. Then, there exists a bounded positive function $\mu_2(y(t), x_r(t), e_s(t))$, $t \geq 0$, such that $\mu_2(y(t), x_r(t), e_s(t)) \geq |\mathbf{e}^T A_r(t) \tilde{e}(t)| + |\mathbf{e}^T f(x(t), h(u(t)), d(t))|$, $t \geq 0$, and, for $\beta(y(t), x_r(t), e_s(t)) = \mu_2(y(t), x_r(t), e_s(t)) + \kappa_2$, $t \geq 0$, where $\kappa_2 > 0$, the zero solution $s(\tilde{e}(t)) \equiv 0$ to the closed-loop system (43) is uniformly finite-time stable and $y(t) - y_r(t) \rightarrow y_s(t)$ in finite time.

Proof: Consider the Lyapunov function candidate given by Equation (49) and note that, using Equations (43) and (59), it follows that the derivative of $V(s(\tilde{e}))$ along the closed-loop system trajectories of \mathcal{G} is given by

$$\begin{aligned} \dot{V}(s(\tilde{e}(t))) &= s(\tilde{e}(t)) \dot{s}(\tilde{e}(t)) \\ &= s(\tilde{e}(t)) [\mathbf{e}^T A_r(t) \tilde{e}(t) + \mathbf{e}^T f(x(t), h(u(t)), d(t)) \\ &\quad - \beta(y(t), x_r(t), e_s(t)) \operatorname{sgn}(s(\tilde{e}(t)))] \\ &\leq |s(\tilde{e}(t))| [|\mathbf{e}^T A_r(t) \tilde{e}(t)| + |\mathbf{e}^T f(x(t), h(u(t)), d(t))| \\ &\quad - \beta(y(t), x_r(t), e_s(t))], \quad t \geq 0. \quad (60) \end{aligned}$$

Since $h(u(t))$, $t \geq 0$, and $d(t)$, $t \geq 0$, are bounded, it follows from Proposition 2.1 and Equation (28) that $x(t)$, $t \geq 0$, is bounded. Hence, $y(t)$, $t \geq 0$, and $f(x(t), h(u(t)), d(t))$,

$t \geq 0$, are bounded. From Proposition 2.1 and Equation (39), it follows that $e_s(t)$, $t \geq 0$, is bounded, and hence, we can choose a bounded positive function $\mu_2(y(t), x_r(t), e_s(t))$, $t \geq 0$, such that

$$\begin{aligned} \mu_2(y(t), x_r(t), e_s(t)) &= \|\mathbf{e}^T A_r(t)\| (\|y(t) + \|x_r(t)\| + \|e_s(t)\|) \\ &\quad + \|\mathbf{e}^T\| (\|A^*\| \|y(t) + \|B^*\| \|h(u(t))\| \\ &\quad + (|\mathbf{e}^T \hat{B}(t)| + \|\mathbf{e}^T\| \|B^*\|) d^*) \\ &\geq \|\mathbf{e}^T A_r(t)\| (\|x(t)\| + \|x_r(t)\| \\ &\quad + \|e_s(t)\|) + \mathbf{e}^T (\|\Delta A(t)\| \|x(t)\| \\ &\quad + \|\Delta B(t)\| \|h(u(t))\|) + (|\mathbf{e}^T \hat{B}(t)| \\ &\quad + \|\mathbf{e}^T\| \|\Delta B(t)\|) d^* \\ &\geq |\mathbf{e}^T A_r(t) \tilde{e}(t)| + |\mathbf{e}^T f(x(t), h(u(t)), d(t))|, \quad t \geq 0. \quad (61) \end{aligned}$$

Next, it follows from Equations (60) and (61) that

$$\begin{aligned} \dot{V}(s(\tilde{e}(t))) &\leq -(\beta(y(t), x_r(t), e_s(t)) \\ &\quad - \mu_2(y(t), x_r(t), e_s(t))) |s(\tilde{e}(t))| \\ &= -\sqrt{2} (\beta(y(t), x_r(t), e_s(t)) \\ &\quad - \mu_2(y(t), x_r(t), e_s(t))) (V(s(\tilde{e}(t))))^{\frac{1}{2}}, \quad t \geq 0, \quad (62) \end{aligned}$$

and for $\beta(y(t), x_r(t), e_s(t)) = \mu_2(y(t), x_r(t), e_s(t)) + \kappa_2$, $t \geq 0$,

$$\dot{V}(s(\tilde{e}(t))) \leq -\sqrt{2} \kappa_2 (V(s(\tilde{e}(t))))^{\frac{1}{2}}, \quad t \geq 0. \quad (63)$$

Thus, it follows from Theorem 13.2 of Haddad et al. (2009, p. 144) that the zero solution $s(\tilde{e}(t)) \equiv 0$ to the closed-loop system (43) with control input given by Equations (36), (37), and (59) is uniformly finite-time stable, and hence, $y(t) - y_r(t) \rightarrow y_s(t)$ in finite time. \square

Note that the controller $u(t)$, $t \geq 0$, is discontinuous due to the presence of signum function $\operatorname{sgn}(s)$ in the controller architecture. This discontinuity can lead to a chattering phenomenon, which is undesirable in practice. In order to reduce or eliminate the chattering effect, a saturation function is generally implemented instead of the signum function, that is, $\operatorname{sgn}(s)$ is replaced by $\operatorname{sat}(s/\Phi)$, where

$$\operatorname{sat}(s/\Phi) \triangleq \begin{cases} -1, & \frac{s}{\Phi} < -1, \\ \frac{s}{\Phi}, & |\frac{s}{\Phi}| \leq 1, \\ 1, & \frac{s}{\Phi} > 1, \end{cases}$$

and $\Phi > 0$ is the boundary layer thickness (Slotine & Li, 1991).

If $\text{sgn}(s)$ is replaced by $\text{sat}(s/\Phi)$, then it follows from Equation (60) that

$$\begin{aligned} \dot{V}(s(\tilde{e}(t))) &= s(\tilde{e}(t))\dot{s}(\tilde{e}(t)) \\ &= s(\tilde{e}(t)) \left[\mathbf{e}^T A_r(t) \tilde{e}(t) + \mathbf{e}^T f(x(t), h(u(t)), d(t)) \right. \\ &\quad \left. - \beta(y(t), x_r(t), e_s(t)) \text{sat}\left(\frac{s(\tilde{e}(t))}{\Phi}\right) \right] \\ &\leq |s(\tilde{e}(t))| \left[|\mathbf{e}^T A_r(t) \tilde{e}(t)| + |\mathbf{e}^T f(x(t), h(u(t)))| \right] \\ &\quad - \beta(y(t), x_r(t), e_s(t)) s(\tilde{e}(t)) \text{sat}\left(\frac{s(\tilde{e}(t))}{\Phi}\right), \\ &\quad t \geq 0. \quad (64) \end{aligned}$$

In this case, outside the boundary layer (i.e., $|\frac{s}{\Phi}| > 1$), $s(\tilde{e}) \text{sat}(\frac{s(\tilde{e})}{\Phi}) = |s(\tilde{e})|$. Therefore,

$$\begin{aligned} \dot{V}(s(\tilde{e}(t))) &\leq |s(\tilde{e}(t))| \left[|\mathbf{e}^T A_r(t) \tilde{e}(t)| \right. \\ &\quad \left. + |\mathbf{e}^T f(x(t), h(u(t)))| \right] \\ &\quad - \beta(y(t), x_r(t), e_s(t)) |s(\tilde{e}(t))| \\ &\leq -(\beta(y(t), x_r(t), e_s(t)) \\ &\quad - \mu_2(y(t), x_r(t), e_s(t))) |s(\tilde{e}(t))| \\ &= -\sqrt{2}\kappa_2 (V(s(\tilde{e}(t))))^{\frac{1}{2}}, \quad t \geq 0. \quad (65) \end{aligned}$$

Hence, for any trajectory starting outside the boundary layer, the controller guarantees that $s(\tilde{e}(t))$, $t \geq 0$, is decreasing until it reaches the set $\{|s(\tilde{e})| \leq \Phi\}$ in finite time and remains inside thereafter. Note that in this case, $s(\tilde{e}(t))$, $t \geq 0$, does not converge to zero but rather remains within the boundary layer, that is, $|s(\tilde{e}(t))| \leq \Phi$. By choosing a sufficiently small value for Φ , $s(\tilde{e}(t))$, $t \geq 0$, can be kept sufficiently close to zero.

Remark 3.3: The proposed controllers in Sections 3.1 and 3.2 are easy to implement since they only require $x_r(t)$, $t \geq 0$, $e_s(t)$, $t \geq 0$, and the sign of $\tilde{e}(t)$, $t \geq 0$, which can be easily obtained from Equations (31), (39), and (42), respectively. The output $y(t)$, $t \geq 0$, can be measured by a spirometer as discussed in Kramme et al. (2011). The controllers do not require significant computational effort in calculating the input pressures, and hence, can be easily implemented with simple microchip controllers.

4. Illustrative numerical example

In this section, we apply the sliding mode controller developed in Section 3 to a two-compartment lung model. The expiratory resistance is typically higher than the inspiratory resistance by a factor of 2–3 (Chellaboina et al., 2010). Here, we assume that the factor is 2. Specifically, we choose the nominal values of parameters to be $\hat{R}_{0,1}^{\text{in}} = 9$ cm H₂O/l/sec, $\hat{R}_{1,1}^{\text{in}} = 16$ cm H₂O/l/sec, $\hat{R}_{1,2}^{\text{in}} = 16$ cm H₂O/l/sec, $\hat{R}_{0,1}^{\text{ex}} = 18$ cm H₂O/l/sec,

$\hat{R}_{1,1}^{\text{ex}} = 32$ cm H₂O/l/sec, and $\hat{R}_{1,2}^{\text{ex}} = 32$ cm H₂O/l/sec. A typical value of the lung compliance is 0.1l/cm H₂O. The inspiration time is $T_{\text{in}} = 2$ sec and the expiration time is $T_{\text{ex}} = 3$ sec. Initial values are set at $x_0^{\text{in}} = [0.5, 0]^T$ l and $x_{r0} = [1, 0.5]^T$ l. The parameters of the reference model are set at $A_r(t) = \hat{A}(t)$, $t \geq 0$, $B_r(t) = 0.6\hat{B}(t)$, $t \geq 0$, $r(t) = 15$ cm H₂O during inspiration, $r(t) = 5$ cm H₂O during expiration, $k_y = 0$, and $k_r = 0.6$. The maximum input pressure is set at $u_{\text{max}} = 19$ cm H₂O.

4.1 System with matched uncertainty

In the first simulation, we assume that the matching condition (44) holds. Specifically, the system uncertainty and system disturbance are given by

$$\begin{aligned} f(x(t), h(u(t)), d(t)) &= \Delta A(t)x(t) + \Delta B(t)h(u(t)) \\ &\quad + B(t) \sin(t), \quad (66) \end{aligned}$$

where $\Delta A(t) = \hat{B}(t)[0.5, 0.5]$ and $\Delta B(t) = 0.5\hat{B}(t)$. Therefore,

$$f(x, h(u), d) = \hat{B}\psi(x, h(u)) + Bd, \quad (67)$$

where $\psi(x, h(u)) = [0.5, 0.5]x + 0.5h(u) = 0.5y + 0.5h(u)$. The bound on $\psi(\cdot, \cdot)$ is given by $|\psi(x, h(u))| \leq kh(u) + \alpha(y)$, where $k = 0.5$ and $\alpha(y) = 0.5y$. The controller gain is set at $\kappa_1 = 0.1$. Figure 2 shows the trajectory of the reference signal as well as the trajectory of the total volume of the lungs as a function of time. Although the system is capable of tracking the desired trajectory, the chattering effect of the sliding mode controller can be clearly seen in Figure 2.

Next, to reduce the chattering phenomenon, we replace the signum function $\text{sgn}(s)$ in Equation (46) with $\text{sat}(s/\Phi)$, where Φ is set to 0.03. As can be seen from Figure 3, this modification in the controller architecture achieves the same tracking performance as in the case of the discontinuous control input without any chattering effect. For the remainder of the simulations, we replace the term $\text{sgn}(s)$ with $\text{sat}(s/\Phi)$.

4.2 System with unmatched uncertainty

In this simulation, we assume that the system uncertainty and system disturbances are given by $f(x(t), h(u(t))) = \Delta A(t)x(t) + \Delta B(t)h(u(t)) + B(t)\sin(t)$, where $\Delta A(t) = 0.5\hat{A}(t)$ and $\Delta B(t) = 0.5\hat{B}(t)$. The controller gain is set at $\kappa_2 = 0.2$ and Φ is set to 0.03. As can be seen from Figure 4, the proposed controller tracks the reference trajectory in the presence of unmatched parameter uncertainty and system disturbances.

In order to test the robustness of the controller, the uncertainty in the system is increased by setting $\Delta A(t) =$

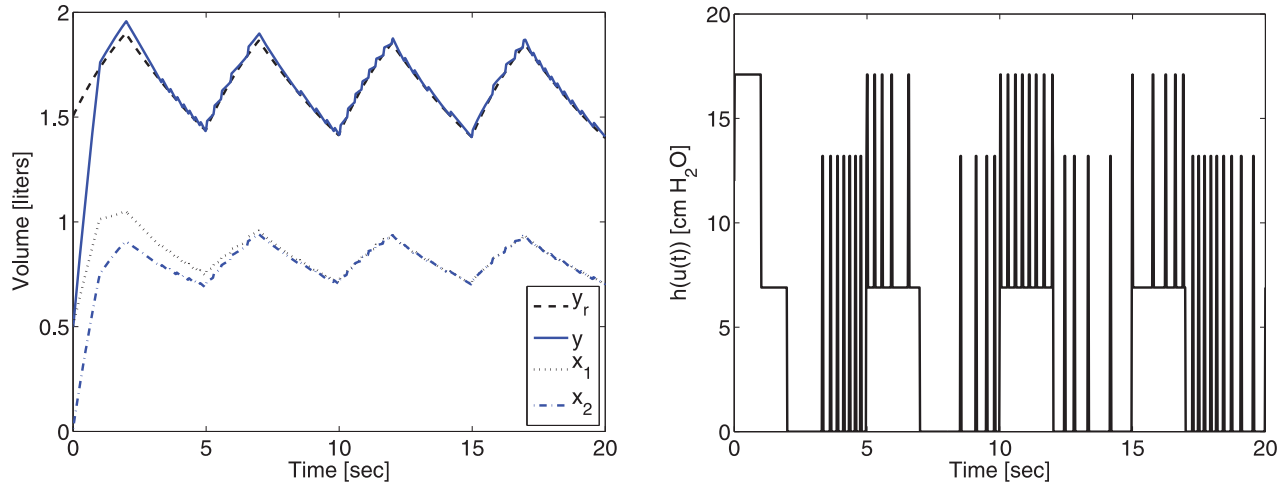


Figure 2. Trajectory tracking for system with matched uncertainty using discontinuous control input.

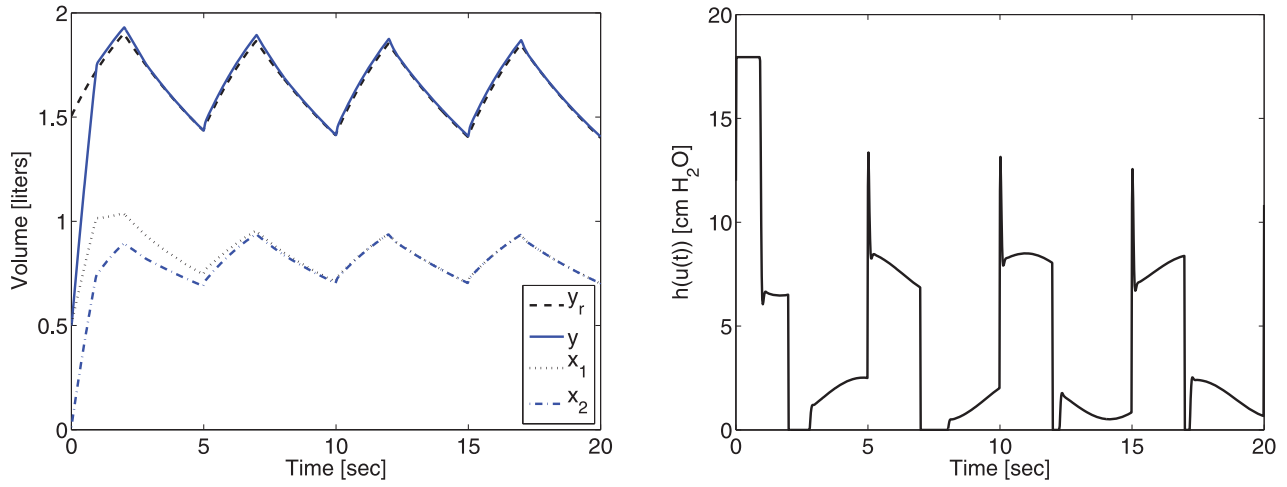


Figure 3. Trajectory tracking for system with matched uncertainty using continuous control input.

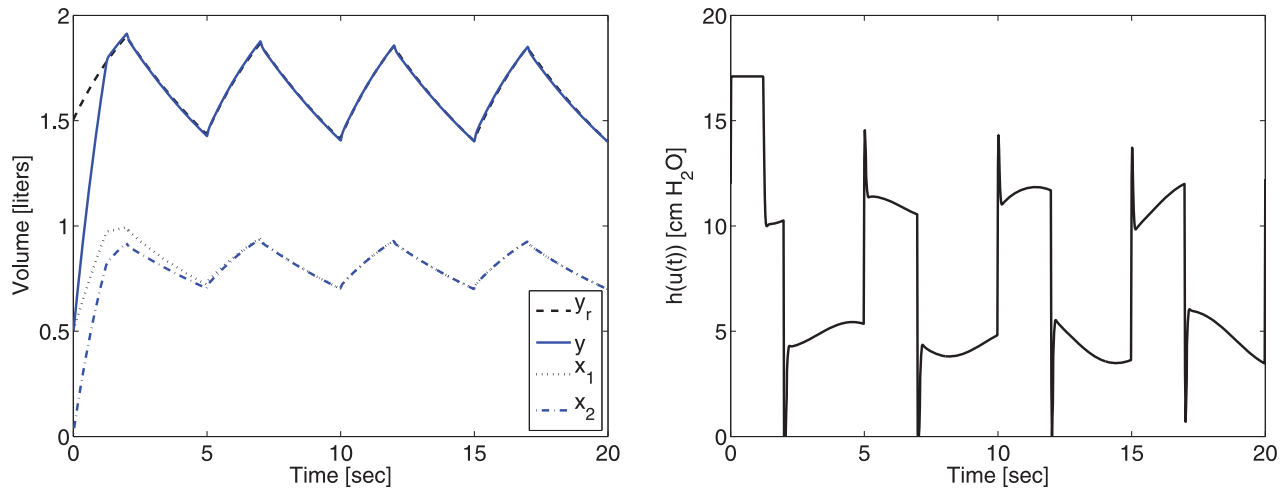


Figure 4. Trajectory tracking for system with unmatched uncertainty.

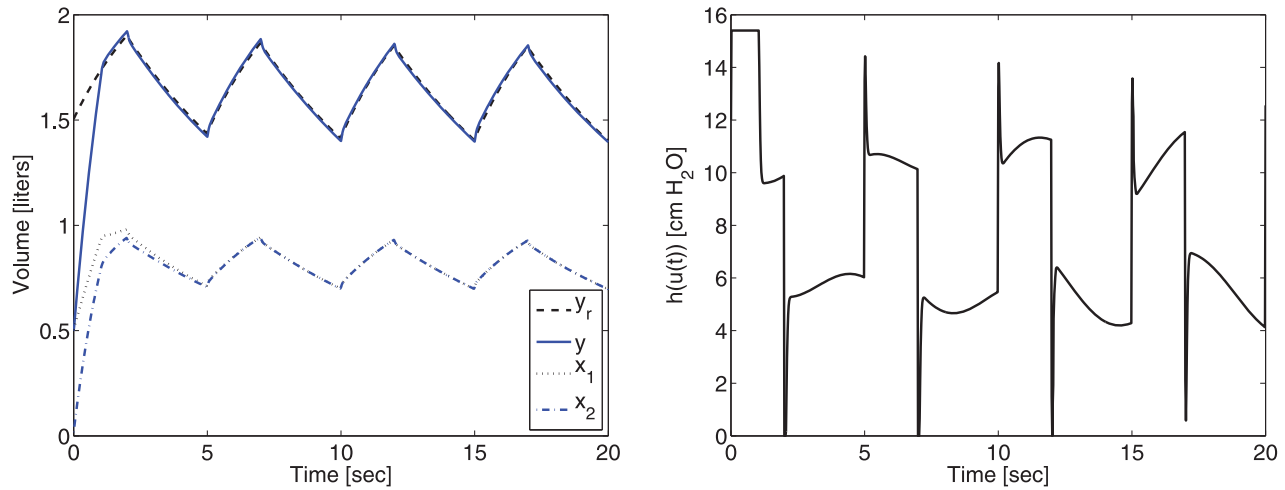


Figure 5. Trajectory tracking for system with large unmatched uncertainty.

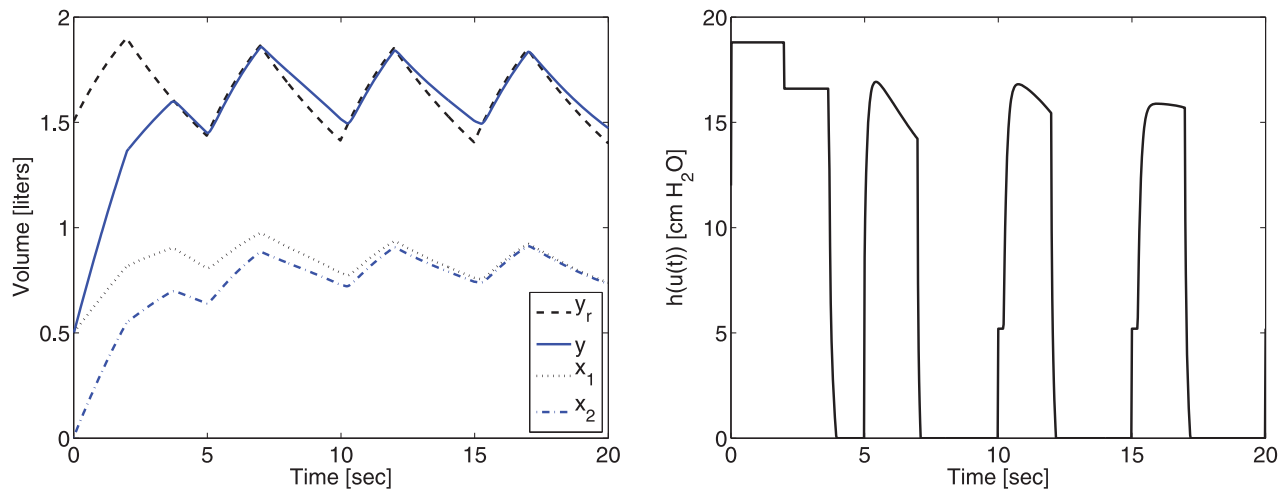


Figure 6. Trajectory tracking when the required control input $u(t)$ for perfect tracking is negative.

$\hat{A}(t)$ and $\Delta B(t) = \hat{B}(t)$. The controller gain is set at $\kappa_2 = 0.2$ and the value of Φ is set to 0.03. As can be seen from Figure 5, the system tracks the reference signal in the presence of large unmatched parameter uncertainty and system disturbances.

Finally, to further elucidate the robustness of the proposed approach, the uncertainty in the system parameters are set to $\Delta A(t) = -0.5\hat{A}(t)$ and $\Delta B(t) = -0.5\hat{B}(t)$. In this case, the controller gain is set at $\kappa_2 = 0.3$ and the value of Φ is set to 0.03. Note that these uncertainties reflect the fact that the actual system is discharging slower than the reference system during the expiration phase. Therefore, in order for the system trajectory to track the desired trajectory, a negative control input $u(t)$, $t \geq 0$, must be applied. In this case, $\Delta h(u(t)) \neq 0$ and as a result $y_s(t) \neq 0$. Thus, a bounded tracking error will result during the expiration phase. This is illustrated in Figure 6.

5. Conclusion

In this paper, we developed a sliding mode control architecture to control lung volume and minute ventilation in the presence of modelling uncertainties. The proposed control framework accounts for the input pressure constraints in the presence of both matched and unmatched system uncertainties and system disturbances. Several illustrative numerical examples were presented to show the efficacy of the proposed control framework. To account for lung compliance variations as a function of lung volume, in future research, we propose to extend the proposed control framework to address nonlinear compartmental dynamical models.

Funding

This publication was made possible by NPRP [grant number 4-187-2-060] from Qatar National Research Fund (a member of

Qatar Foundation). The statements made herein are solely the responsibility of the authors.

References

- Chellaboina, V., Haddad, W.M., Li, H., & Bailey, J.M. (2010). Limit cycle stability analysis and adaptive control of a multi-compartment model for a pressure-limited respirator and lung mechanics system. *International Journal of Control*, 83(5), 940–955.
- Dojat, M., Brochard, L., Lemaire, F., & Harf, A. (1992). A knowledge-based system for assisted ventilation of patients in intensive care units. *International Journal of Clinical Monitoring and Computing*, 9(4), 239–250.
- Edwards, C., & Spurgeon, S.K. (1998). *Sliding mode control: Theory and applications*. New York, NY: Taylor & Francis.
- Haddad, W.M., Nersesov, S.G., & Du, L. (2009). Finite-time stability for time-varying nonlinear dynamical systems. In S. Sivasundaram, J.V. Devi, Z. Drici, & F. Mcrae (Eds.), *Advances in nonlinear analysis: Theory methods and application* (pp. 139–150). Cambridge, UK: Cambridge Scientific Publishers.
- Kramme, R., Hoffmann, K.-P., & Pozos, R.S. (2011). *Springer handbook of medical technology*. Berlin-Heidelberg: Springer-Verlag.
- Laubscher, T., Heinrichs, W., Weiler, N., Hartmann, G., & Brunner, J. (1994). An adaptive lung ventilation controller. *IEEE Transactions on Biomedical Engineering*, 41(1), 51–59.
- Li, H., & Haddad, W.M. (2013). Model predictive control for a multicompartment respiratory system. *IEEE Transactions on Control Systems Technology*, 21(5), 1988–1995.
- Martin, L. (1987). *Pulmonary physiology in clinical practice*. St. Louis, MO: Mosby.
- McLuckie, A. (2004). Editorial II: High-frequency oscillation in acute respiratory distress syndrome (ARDS). *British Journal of Anaesthesia*, 93(3), 322–324.
- Medoff, B.D., Harris, R.S., Kesselman, H., Venegas, J., Amato, M.B., & Hess, D. (2000). Use of recruitment maneuvers and high positive end-expiratory pressure in a patient with acute respiratory distress syndrome. *Critical Care Medicine*, 28(4), 1210–1216.
- Nunes, E., Hsu, L., & Lizarralde, F. (2009). Global exact tracking for uncertain systems using output-feedback sliding mode control. *IEEE Transactions on Automatic Control*, 54(5), 1141–1147.
- Sinderby, C., Navalesi, P., Beck, J., Skrobik, Y., Comtois, N., Friberg, S., . . . Lindstrom, L. (1999). Neural control of mechanical ventilation in respiratory failure. *Nature Medicine*, 5(12), 1433–1436.
- Slotine, J.J.E., & Li, W. (1991). *Applied nonlinear control*. Englewood Cliffs, NJ: Prentice-Hall.
- Tao, G. (2003). *Adaptive control design and analysis*. New York, NY: Wiley.
- Tobin, M.J. (1994). *Principles and practice of mechanical ventilation*. New York, NY: McGraw-Hill.
- Utkin, V. (1977). Variable structure systems with sliding modes. *IEEE Transactions on Automatic Control*, 22(2), 212–222.
- Volyanskyy, K., Haddad, W., & Bailey, J. (2011). Pressure-and work-limited neuroadaptive control for mechanical ventilation of critical care patients. *IEEE Transactions on Neural Networks*, 22(4), 614–626.
- Weibel, E.R. (1963). *Morphometry of the human lung*. New York, NY: Academic.
- West, J.B. (2008). *Respiratory physiology: The essentials*. Baltimore, MD: Lippincott Williams & Wilkins.
- Younes, M., Puddy, A., Roberts, D., Light, R., Quesada, A., Taylor, K., . . . Cramp, H. (1992). Proportional assist ventilation: Results of an initial clinical trial. *American Review of Respiratory Disease*, 145(1), 121–129.
- Zhang, J., & Xia, Y. (2010). Design of static output feedback sliding mode control for uncertain linear systems. *IEEE Transactions on Industrial Electronics*, 57(6), 2161–2170.